Active adaptive sound control in a duct: A computer simulation

J. C. Burgess[a)]

Acoustics Research Department, Bell Laboratories, Murray Hill, New Jersey 07974
(Received 9 February 1981; accepted for publication 2 June 1981)

Most active sound cancellation systems reported in the literature use open-loop control, depend on near-zero phase delay in control system elements, and require constant acoustic signal transit time from a signal pickup (microphone) to a control sound source (loudspeaker). The applicability of such systems can be significantly enhanced by using closed-loop control. This study concerns a digital computer simulation of adaptive closed-loop control for a specific application, sound cancellation in a duct. The key element is an extension of Sondhi's adaptive echo canceler and Widrow's adaptive noise canceler from signal processing to control. The adaptive algorithm is thus based on the LMS gradient search method. The simulation shows that one or more pure tones can be canceled down to the computer bit noise level (— 120 dB). In the presence of additive white noise, pure tones can be canceled to at least 10 dB below the noise spectrum level for SNR's down to at least 0 dB. The underlying theory implies that the algorithm allows tracking tones with amplitudes and frequencies that change more slowly with time than the adaptive filter adaptation rate. The theory implies also that the method can cancel narrow-band sound in the presence of spectrally overlapping broadband sound. The method can be applied more widely, particularly to control systems that involve transport delay.

PACS numbers: 43.60. — c, 43.20.Mv, 43.20.Hq, 43.50.Gf

INTRODUCTION

Helmholtz resonators have long been used to control sound.[1] An active counterpart to the Helmholtz resonator was first described by Olson in 1953.[2] Tartakovsky in 1968,[3] Jessel and Mangiante in 1972,[4] and Swinbanks in 1973[5] described the start of currently ongoing efforts in active sound control in Europe. Canévet and Mangiante,[6] Leventhall,[7] and Poole and Leventhall[8,9] discussed active control of sound in ducts. The Swinbanks–Leventhall work is further described in a technical note[10] and a patent.[11] Mangiante[12] and Angevine[13] have described extension of active sound control to three-dimensional systems. Angelini and Capolino[14] discussed briefly the application of optimum filtering (time-continuous Wiener–Hopf method) to active sound reduction.

The active sound control devices described in the papers just cited consist principally of one or more microphones, amplifiers with bulk delay, and one or more loudspeakers to provide out-of-phase sound. All have open-loop control. Among the important requirements for satisfactory operation placed on the total system by open-loop control are (1) control system components must have nearly zero phase delay over the frequency range of operation, and (2) uncontrolled system parameters (e.g., temperature, flow rate in ducts) must be nearly constant, so that they do not affect significantly the time of sound transmission between microphone(s) and loudspeaker(s). In practice, real control systems will have nonzero, frequency-dependent phase delay, and real uncontrolled system parameters will change with time. These practical problems can result in at least decreased effectiveness and at worst amplification of sound (ringing) rather than attenuation.

Onoda and Kido[15] have reported the only adaptive active sound control system known to the author. (Adaptive, as used in this paper, denotes a closed-loop system with learning capability; i.e., a system which has the capability to change system parameters.) The system as reported is limited to canceling a single pure tone. The method uses one form of a gradient search to find the appropriate amplitude and phase.

The method for active sound control described in the present paper is adaptive and broadband. It is an application and extension of the adaptive echo canceler reported by Sondhi[16] and the adaptive noise canceler reported by Widrow *et al.*[17] The paper describes the theory and operation (computer simulation) of the system applied to sound transmission in a duct. With respect to the method used by Sondhi and Widrow, the present work is an extension from adaptive signal processing to adaptive control. The essential difference is that the adaptive control system involves fixed transfer functions (gains and phase delays) that are not important in signal processing systems. With respect to Onoda and Kido's method, the present work is an extension to multiple tones. In addition, it is based on a well-known, proven, and easy-to-implement least-mean-square (LMS) gradient search algorithm. The method allows extension of the work described by Jessel, Mangiante, Swinbanks, and Leventhall to systems with uncontrolled, gradually changing parameters.

The method depends upon an intriguing kind of filtering. It distinguishes between components of a signal on the basis of bandwidth, not on where the energy lies in the frequency band. Thus it can converge on a narrow-band signal in the presence of a broadband signal with an overlapping spectrum. When the estimate of the narrow-band signal is subtracted from the broadband signal, the result is that separate estimates are available of both the broadband and narrow-band signals.

The method is not without its limitations. It requires a "training" signal which must be correlated with (not necessarily identical to) the narrow-band portion of the

a)Present address: Department of Mechanical Engineering, University of Hawaii, Honolulu, HI 96822.

 0001-4966/81/090715-12$00.80 © 1981 Acoustical Society of America

Redistribution subject to ASA license or copyright; see http://acousticalsociety.org/content/terms. Download to IP: 132.174.255.116 On: Thu, 27 Nov 2014 08:02:32

total signal. ["Training" is used for a lack of a better word. The training signal x_k (see Fig. 3) has two functions. It is necessary to and limits the ability of the adaptive filter to "learn" what coefficient values it should have. It is also the input signal on which the adaptive filter operates.] The system is capable of attenuating white noise only if the control system has zero phase delay, and if the training signal has all the frequency components of the sound to be attenuated.

The problem addressed in this paper is cancellation of the zeroth-order mode of sound propagation in a duct by a controlled monopole source. The results presented are intended to show by computer simulation that active adaptive sound control is feasible and effective for this application.

A principal purpose of this paper is to show that adaptive signal processing techniques can be extended to control. The author believes these results will prove valid in practice, but such proof has yet to be given. The author believes the method has far wider application to problems of active equalization and control. In particular, the simulation is an example of the application of adaptive control to problems involving transport delay.

I. ACTIVE "HELMHOLTZ RESONATOR"

The theory of a Helmholtz resonator is well known.[18,19] Some behavioral aspects are important to adaptive sound control. Consider a Helmholtz resonator used as a side branch in an otherwise reflectionless duct (Fig. 1). The resonator responds to an incident wave by acting as a source. We define a perfect source as one with no internal damping and a natural frequency equal to that of an incident harmonic wave. The perfect source then generates two waves equal in amplitude to the incident wave, one positive-going, the other negative-going.

On the positive-going side of the resonator, the source-generated pressure and volume velocity cancel those of the incident wave. On the negative-going side, the two waves combine to form standing waves. The standing waves have a pressure node and a volume velocity antinode at the resonator location.

When acting as a perfect source in a duct, a Helmholtz resonator is most easily visualized as a volume velocity source. The source strength required is set by the volume velocity in the incident wave. As the preceding discussion shows, the perfect source can be conceived also as a pressure source even though the total pressure is zero at the source location.

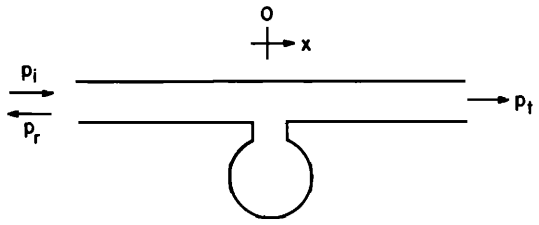

FIG. 1. Passive Helmholtz resonator as a side branch in a duct.

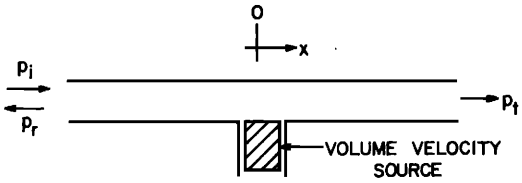

FIG. 2. Active "Helmholtz resonator" as a side branch in a duct.

For an active "Helmholtz resonator," we replace the passive resonator elements by a volume velocity source (Fig. 2). Such a device is a monopole source (see, e.g., Leventhall[7]). When operating perfectly, the strength requirement is identical to that for the passive resonator. If the amplitude and phase of the source can be properly controlled, the active device will perform exactly as the passive device in the perfect case.

The active "Helmholtz resonator" has a distinct advantage over the passive resonator. It can be controlled to act at any reasonable number of frequencies, and it can be controlled to act perfectly (or, in practice, nearly so). A single monopole source can thus replace a number of passive resonators.

II. ADAPTIVE NOISE CANCELER

The adaptive sound control system described in this paper is based on the adaptive echo canceler[16,20] and the adaptive noise canceler.[17] It is generically related to the adaptive line enhancer.[17,21] We will use ANC in this paper to refer to all of these. Since the theory of operation of the ANC is well described elsewhere,[16,17,20-22] only a brief review is given here. The discussion is further limited to time-discrete systems, although the underlying theory is applicable to time-continuous systems as well.[16,20] The ANC is a signal processing application. All signals are normally voltages, and power controlled is generally insignificant.

Figure 3 shows the ANC together with some of the nomenclature used in this paper (ur is a single variable, not a product). The subscript k represents discrete time, $t_k = kT_s$, where T_s is the sampling interval (i.e., $k = t_k/T_s$ is *normalized discrete time*). The essential difference between the narrow-band signal, s_k, and the broadband noise, n_k, is the length of time (autocorrelation time) over which the signal components exhibit significant autocorrelation values. When the time delay Δ (decorrelation delay) is taken greater than the autocorrelation time of n_k, the training signal x_k

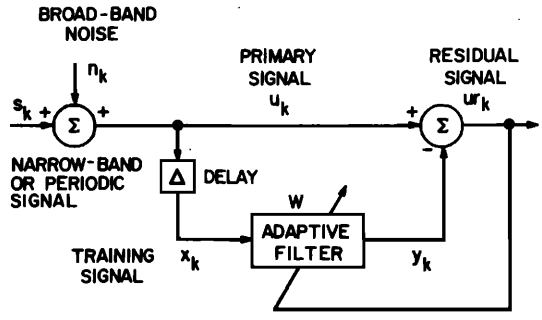

FIG. 3. Adaptive noise canceler (ANC).

Redistribution subject to ASA license or copyright; see http://acousticalsociety.org/content/terms. Download to IP: 132.174.255.116 On: Thu, 27 Nov 2014 08:02:32

can be taken as uncorrelated with the broadband component of the primary signal u_k. A necessary assumption is that Δ is short enough that x_k remains correlated with the narrow-band components of u_k.

We use the following terminology (following Treichler[21] with modifications):

$\mathbf{U}_k \triangleq [u_k\, u_{k-1} \cdots u_{k-L+1}]^T$ = vector of present and past signal values,

$\mathbf{W}_k \triangleq [w_{k,0} w_{k,1} \cdots w_{k,L-1}]^T$ = vector of filter coefficients at time k,

$\mathbf{R}_u \triangleq E\{\mathbf{U}_{k-\Delta}\mathbf{U}_{k-\Delta}^T\}$ = autocorrelation matrix for signal u_k,

$\mathbf{P}_{u,\Delta} \triangleq E\{u_k\mathbf{U}_{k-\Delta}\}$ = autocorrelation vector for signal u_k,

where E denotes "expected value of." For the purpose of the following discussion, we take s_k as a correlated stationary random process and n_k as a zero mean white stationary random process. Computer simulation shows that the final results are at least good approximations for s_k a periodic process, as well.

The usual realization of the adaptive filter W, and the one used here, is a tapped delay line of length L (Fig. 4). The output is

$$y_k = \sum_{l=0}^{L-1} w_{k,l} x_{k-l} = \mathbf{W}_k^T \mathbf{X}_k = \mathbf{X}_k^T \mathbf{W}_k . \tag{1}$$

W is thus an FIR filter, and its output is a weighted moving average of the input.

At any time k, the system operating equations consist of Eq. (1) together with (Fig. 3)

$$x_k = u_{k-\Delta}, \tag{2}$$

$$ur_k = u_k - y_k . \tag{3}$$

Using Eqs. (1) and (2), Eq. (3) becomes

$$ur_k = u_k - \mathbf{W}_k^T\mathbf{U}_{k-\Delta} = u_k - \mathbf{U}_{k-\Delta}^T\mathbf{W}_k . \tag{4}$$

The mean-square residual (error) is

$$\begin{aligned} E\{ur_k^2\} &= E\{u_k^2\} - 2\mathbf{W}_k^T E\{u_k\mathbf{U}_{k-\Delta}\} + \mathbf{W}_k^T E\{\mathbf{U}_{k-\Delta}\mathbf{U}_{k-\Delta}^T\}\mathbf{W}_k \\ &= r_{u,0} - 2\mathbf{W}_k^T\mathbf{P}_{u,\Delta} + \mathbf{W}_k^T\mathbf{R}_u\mathbf{W}_k . \end{aligned} \tag{5}$$

The reason for calling Δ a decorrelation delay can be seen by examining the autocorrelation vector $\mathbf{P}_{u,\Delta}$. Using $u_k = s_k + n_k$ (Fig. 1), we have (for $\Delta \geq 1$)

$$\mathbf{P}_{u,\Delta} = E\{u_k\mathbf{U}_{k-\Delta}\} = E\{s_k\mathbf{S}_{k-\Delta}\} = \mathbf{P}_{s,\Delta}, \tag{6}$$

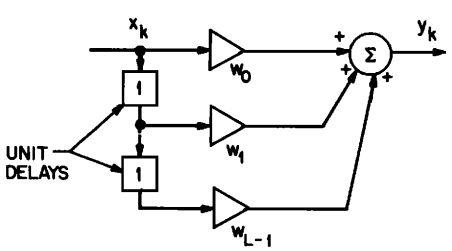

FIG. 4. Tapped delay line (FIR filter) of length L.

since, by definition of s_k and n_k,

$E\{s_k n_j\} = 0$, for all k, j,

$E\{n_k n_j\} = 0$, for all $k \neq j$.

Thus Δ causes the autocorrelation vector $\mathbf{P}_{u,\Delta}$ to be, in reality, the autocorrelation vector of only the relatively coherent (narrow-band) component of u_k.

The gradient of the mean-square residual "performance surface,"[22] Eq. (5), taken with respect to the filter coefficients $w_{k,l}$, is

$$\nabla E\{ur_k^2\} = -2\mathbf{P}_{u,\Delta} + 2\mathbf{R}_u\mathbf{W}_k . \tag{7}$$

The optimum filter coefficients in the LMS sense are those for which the gradient is zero. The result of applying this condition is the discrete form of the Wiener–Hopf equation,

$$\mathbf{W}^* = \mathbf{R}_u^{-1}\mathbf{P}_{u,\Delta} . \tag{8}$$

The coefficients w_l^* of the Wiener filter can always be determined off-line by implementing Eq. (8). The process is used extensively in linear predictive coding (LPC) analysis and in the maximum entropy method (MEM) (see, e.g., Childers,[23] particularly the excellent review paper by Makhoul[24]). The direct solution, Eq. (8), represents a batch process, however, while our interest is in an on-line, continuously adaptive process.

Widrow,[22] who traces his introduction of the idea back to 1960, showed that the method of steepest descent can be described by

$$E\{\mathbf{W}_{k+1}\} = E\{\mathbf{W}_k\} - \mu'\nabla E\{ur_k^2\}, \tag{9}$$

where the change in $\mathbf{W}$ is proportional to the negative of the gradient, and μ' is a sufficiently small constant. This leads to Eq. (8) as $k \to \infty$. Both Sondhi[16] and Widrow independently implemented a practical approximation to Eq. (9),

$$\mathbf{W}_{k+1} = \mathbf{W}_k - \mu'\nabla ur_k^2, \tag{10}$$

in which expected values are replaced by current values. Using Eq. (4), Eq. (10) can be put in the form

$$\mathbf{W}_{k+1} = (\mathbf{I} - 2\mu'\mathbf{U}_{k-\Delta}\mathbf{U}_{k-\Delta}^T)\mathbf{W}_k + 2\mu' u_k\mathbf{U}_{k-\Delta} . \tag{11a}$$

By taking expectations and neglecting the covariance between $\mathbf{U}_{k-\Delta}\mathbf{U}_{k-\Delta}^T$ and $\mathbf{W}_k$, Eq. (11a) reduces, as it should, to Eq. (9) with Eq. (7).

While the form of Eq. (11a) has theoretical value, it is easier to implement in another form. By using $\nabla ur_k^2 = 2ur_k\nabla ur_k$, we can write

$$\mathbf{W}_{k+1} = \mathbf{W}_k + 2\mu' ur_k\mathbf{U}_{k-\Delta} . \tag{11b}$$

The arrow through the adaptive filter in Fig. 3 represents updating of the coefficients by Eq. (11b).

Convergence of Eq. (11) has been well discussed in the literature.[16,17,20–22,25,26] One important result is that the filter update algorithm does not converge in the discrete case for all μ', Griffiths[25] has suggested that convergence is assured if

$$0 \leq \mu' \leq 1/LP(x), \tag{12}$$

where L is the length of the adaptive filter, and $P(x)$ is

Redistribution subject to ASA license or copyright; see http://acousticalsociety.org/content/terms. Download to IP: 132.174.255.116 On: Thu, 27 Nov 2014 08:02:32

the average power in the training signal, x_k. Equation (12) shows that the convergence range for μ' is signal dependent.

It would be convenient if we could find a normalized convergence parameter μ such that

$$0 \leq \mu \leq 1. \tag{13}$$

While no means appears yet to be known by which to assure Eq. (13), we can approximate it by using Griffiths' limit from Eq. (12). The normalized algorithm equivalent to Eq. (11b) then becomes

$$\mathbf{W}_{k+1} = \mathbf{W}_k + 2\mu[ur_k \mathbf{U}_{k-\Delta}/LP(x)]. \tag{14a}$$

Equation (14a) has value in computer simulation when the power in u_k is set a *priori*. Sondhi and Berkley[20] have called attention to a variant of Eq. (14a) often used in echo cancelers in which the mean energy, $LP(x)$, is replaced by the actual (time-varying) energy,

$$\mathbf{W}_{k+1} = \mathbf{W}_k + 2\mu[ur_k \mathbf{U}_{k-\Delta}/\mathbf{U}_{k-\Delta}^T \mathbf{U}_{k-\Delta}]. \tag{14b}$$

This form has clear value in practical applications, where the mean power in x_k is not usually known.

III. ADAPTIVE SOUND CONTROLLER

The key element in this paper is an extension of the ANC to an adaptive sound controller (ASC). The acoustic portion of the ASC is shown in Fig. 5. The volume velocity supplied by the active "Helmholtz resonator" (Fig. 2) is $\hat{u}_k$. After adaptation, $\hat{u}_k$ is a "best" out-of-phase estimate of u_k in the sense that it minimizes approximately the mean-square residual volume velocity, ur_k. Note that $\hat{u}_k$ is added with a positive sign. Although this is a necessary physical requirement, it is mathematically only trivially different from subtracting an in-phase estimate (Fig. 3). The signs in Eq. (16) *et seq.* are affected.

There are two essential differences between the ASC and the ANC. One is that the ASC operates on the variable to be controlled via an external power source rather than directly. The second is that the residual error cannot be used directly, but must be sensed by a transducer. The transfer functions for these operations are represented by $H2$ and $H3$ in Fig. 6.

There are two systems, which must be kept distinct (Fig. 6). One is the filtering system, in which the estimate $\hat{u}_k$ is found from $u_{k-\Delta}$. The other is the adaptive filter coefficient update system.

The equations for the filtering system can be written directly from Fig. 6. They are Eqs. (1) and (2) together with

$$\hat{u}_k = h2 * y_k, \tag{15}$$

$$ur_k = u_k + \hat{u}_k, \tag{16}$$

$$\epsilon_k = h3 * ur_k, \tag{17}$$

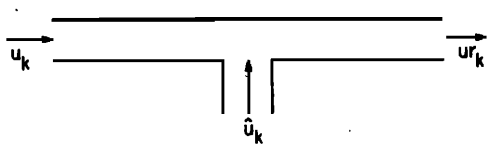

FIG. 5. Acoustic portion of adaptive sound controller.

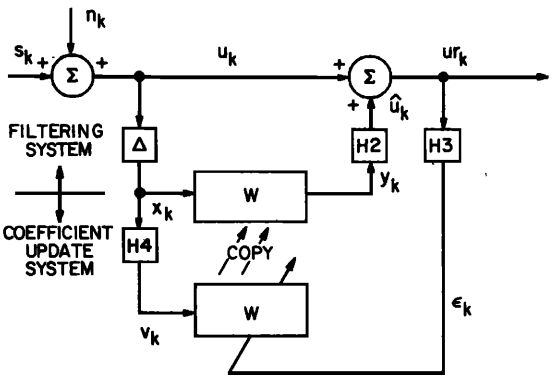

FIG. 6. Schematic for computer simulation of an adaptive sound controller.

where * denotes convolution.

The residual volume velocity can be written in terms of u_k by combining Eqs. (16), (15), (2), and (1),

$$ur_k = u_k + h2 * w_k * u_{k-\Delta}, \tag{18a}$$

where w_k is the impulse response of the adaptive filter at time k. Since W is an FIR filter, the impulse response consists of the L values of $w_{k,l}$, all known at time k. The process of adaptation requires that this impulse response change with time. Thus the corresponding z transform also changes with time. In this discussion, we use nomenclature such as $W_k(z)$ and $\hat{U}_k(z)$ to denote functions during any stage of the adaptation process. We use nomenclature such as $W(z)$ and $\hat{U}(z)$ (no subscript k) to denote functions after adaptation. As the subsequent discussion makes clear, these functions are still time dependent after adaptation, since the adapted coefficients $w_{k,l}$ vary slightly with time about their mean values. While the concept of a time-dependent z transform is valid for the purpose of describing the state of the system at time k, it is only an approximation in describing the filtering process. This approximation (of a time-dependent system by a time-independent system) becomes increasingly less questionable as μ (or μ') $\to 0$, and it is exact in the limit.

Using the z transform, Eq. (18a) becomes

$$UR_k(z) = U(z)[1 + H2(z)W_k(z)z^{-\Delta}]. \tag{18b}$$

We define two useful auxiliary transfer functions,

$$\bar{W}_k(z) = \hat{U}_k(z)/U(z) = H2(z)W_k(z)z^{-\Delta}, \tag{19}$$

$$\bar{H}_k(z) = UR_k(z)/U(z) = 1 + \bar{W}_k(z). \tag{20}$$

$\bar{W}_k$ describes how the primary signal u_k is filtered at time k to obtain the estimate $\hat{u}_k$, while $\bar{H}_k$ describes how u_k is filtered to obtain the residual ur_k. Note that, for the system of Fig. 6, $\bar{W}$ passes some of the uncorrelated noise in x_k.

For the adaptive filter coefficient update system, the signal we have available is ϵ_k, not ur_k. The method of steepest descent using the gradient of the present value of ϵ_k^2 gives

$$\mathbf{W}_{k+1} = \mathbf{W}_k - \mu' \nabla \epsilon_k^2. \tag{21}$$

Using Eqs. (2), (17), and (18), together with $\nabla \epsilon_k^2 = 2\epsilon_k \nabla \epsilon_k$,

Redistribution subject to ASA license or copyright; see http://acousticalsociety.org/content/terms. Download to IP: 132.174.255.116 On: Thu, 27 Nov 2014 08:02:32

we find

$$\mathbf{W}_{k+1} = \mathbf{W}_k - 2\mu' \epsilon_k \mathbf{V}_k , \tag{22a}$$

where (Fig. 6)

$$\nu_k = h4 * x_k , \tag{22b}$$

$$h4 = h2 * h3 . \tag{22c}$$

Equations (22) represent the key theoretical result in this paper. They bear the same relationship to the ASC as Eqs. (11) bear to the ANC. Since $H2$ and $H3$ are passive filters, the convergence properties of both Eqs. (22) and (11) should be similar. The normalized counterparts to Eqs. (14a) and (14b) are

$$\mathbf{W}_{k+1} = \mathbf{W}_k - 2\mu[\epsilon_k \mathbf{V}_k / LP(\nu)] , \tag{23a}$$

$$\mathbf{W}_{k+1} = \mathbf{W}_k - 2\mu[\epsilon_k \mathbf{V}_k / \mathbf{V}_k^T \mathbf{V}_k] , \tag{23b}$$

where $P(\nu)$ is the power in the signal ν_k. The simulation described in Sec. V uses Eq. (23a).

IV. COMMENTS ON APPLICATION

Volume velocity is taken in this paper as the acoustic control variable. This choice is based on the ease with which the control source can be visualized as a volume velocity source. Pressure can also be taken as the acoustic control variable (Sec. I). All references to volume velocity in equations and figures in this paper are interchangeable with acoustic pressure.

Using acoustic pressure as the control variable in a realization has at least two advantages relative to volume velocity. One advantage is the ready availability of rugged, dependable pressure microphones. There is no practical method for measuring volume velocity in a duct. Devices for measuring or estimating particle velocity have well-known drawbacks (e.g., hot wire anemometers cannot sense flow direction, ribbon microphones are delicate, two matched microphone channels are required to sense pressure gradient). The second advantage is that adaptation places a pressure node in the acoustic field at the control source. Control results should not be overly sensitive to microphone location or to three-dimensional effects near the source. This is not true for volume velocity. There is a volume velocity antinode at the control source with volume velocity cancellation "downstream." Three-dimensional flow effects near the source may make control results sensitive to the location of a velocity sensor.

Any realization requires a proper training signal. One possibility is to use microphones in the duct upstream of the volume velocity source.[4-12] To avoid problems with standing waves, two (or more) microphones could be placed a suitable distance apart. The training signal must only be correlated with the signal to be canceled, not identical to it (i.e., phase is not important). The training signal can thus be taken as any linear combination of microphone outputs. If the correlated portion of the sound results from some external action, such as a pump or an engine, the fundamental frequency can be obtained in a number of ways. The training signal can then be formed by generating sinusoids of any amplitude at this fundamental and at as many of its harmonics as desired. This has the advantage that all harmonics in the training signal can be made equal amplitude.

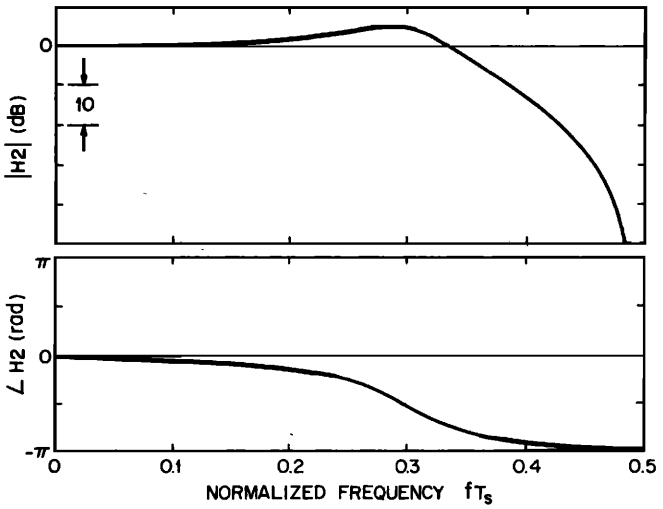

FIG. 7. Frequency response assumed for volume velocity source (transfer function H2).

Another possibility is that the error signal could be used as a training signal. This has the advantage of reducing the number of transducers required. A disadvantage is that the strength of the coherent components in the training signal decreases as the system adapts. As a result, the gain of the adaptive filter W must continually increase. At some point, this "boot-strap" operation breaks down. The possible sound reduction may be limited to small amounts by potential instability (i.e., 10 to 20 dB). It is worth noting that this configuration is similar in its effects to Olson's sound absorber,[2] with the adaptive algorithm replacing Olson's passive Helmholtz resonator and control circuits.

V. COMPUTER SIMULATION: ADAPTIVE PERFORMANCE AND DISCUSSION

The system simulated is shown in Fig. 6. All variables represent time-discrete, uniformly sampled

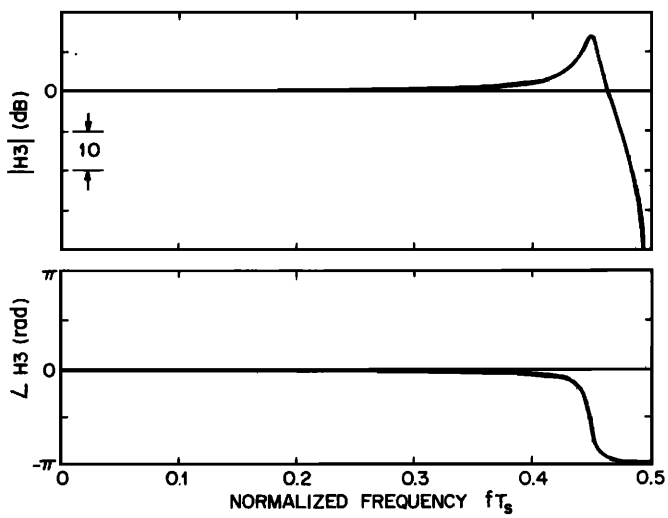

FIG. 8. Frequency response assumed for microphone (transfer function H3).

Redistribution subject to ASA license or copyright; see http://acousticalsociety.org/content/terms. Download to IP: 132.174.255.116 On: Thu, 27 Nov 2014 08:02:32

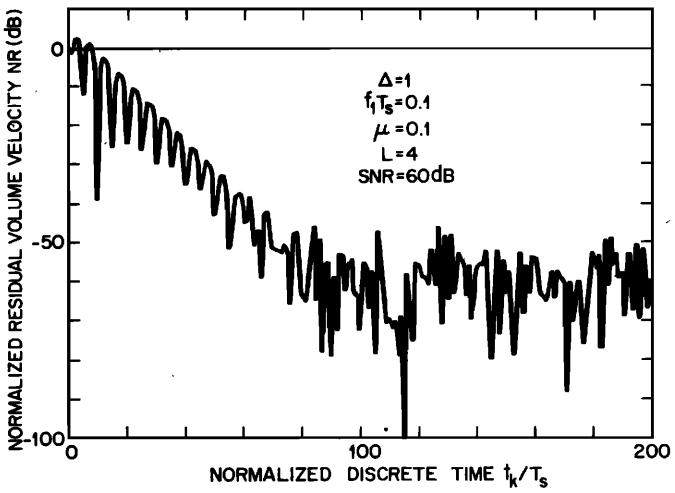

FIG. 9. Typical simulated residual volume velocity versus discrete time; $fT_s = 0.1$.

signals. The system most closely resembles the ASC where the training signal is obtained using microphones upstream of the adaptive "Helmholtz resonator." The simulation was performed on a Data General Eclipse S/250 computer system having a Tektronix 4014 graphics terminal.

The simulated volume velocity u_k consists of one to five sinusoids (called "signal" in this paper) added to white pseudo-random noise, approximately Gaussian, all generated by utility subroutines. The amplitudes and frequencies of the sinusoids and the signal-to-noise ratio (SNR) can be selected as desired. The resulting simulated u_k is normalized so that $u_k(\text{rms}) = 1$. All simulation results presented reflect this normalization.

The purpose of having $H2$ and $H3$ in the simulation is only to explore the effects of their gain and phase on system performance. Both are therefore taken as simple second-order dynamic systems. Using the bilinear transformation, the corresponding IIR digital filters have two zeros at $z = -1$. The two poles were chosen by trial and error so that the resulting frequency response curves could reasonably represent a simple loudspeaker (Fig. 7) and a microphone (Fig. 8). The abscissa for both figures is normalized frequency $f T_s$. Since $1/T_s$ is the sampling rate, $f T_s = 0.5$ corresponds to the Nyquist frequency. Except where otherwise stated, all results presented include the effects of the transfer functions shown in Figs. 7 and 8.

All simulated results are shown for a decorrelation delay $\Delta = 1$. The phase delay in $H4$ acts as an additional, frequency-dependent, decorrelation delay. For the signals simulated, moderate variation in Δ, including $\Delta = 0$, had no significant effect on results.

Convergence of the adaptive process of Fig. 6 with Eq. (23a) has a number of interesting operating characteristics. These include the influence of μ, L, frequency of s_k, SNR, $H2$, and $H3$. These influences are often interrelated. It is convenient to introduce the normalized residual volume velocity in decibels,

$$\text{NR} = 20 \log_{10} ur_k / u_{k,\text{rms}} . \tag{24}$$

After adaptation, NR can be thought of also as noise reduction.

Figures 9 and 10 show examples of convergent behavior when s_k has the normalized frequencies $f_1T_s = 0.1$ and 0.45, respectively. For $f_1T_s = 0.1$, the gain/phase for $H2$ and $H3$ are both near 0 dB/0; for $f_1T_s = 0.45$, they are approximately -27 dB/$-\pi$ and $+15$ dB/-0.5π, respectively. Thus convergence occurs even in the presence of significant gain and phase shifts in $H2$ and $H3$. Simulation, similar to that shown in Fig. 9 but with SNR = 0, shows convergence down to the computer

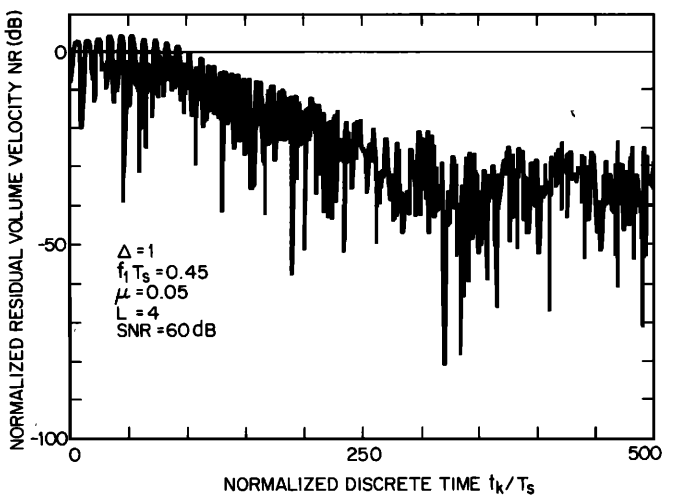

FIG. 10. Typical simulated residual volume velocity versus discrete time; $fT_s = 0.45$.

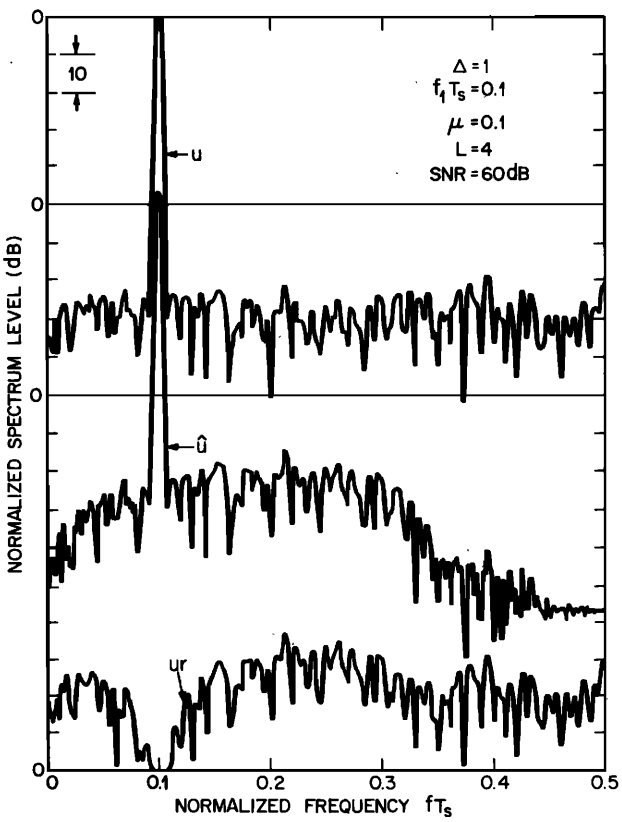

FIG. 11. Adapted FFT spectra of u_k, $\hat{u}_k$, and ur_k for $f_1T_s = 0.1$ (same parameter values as Fig. 10; ordinates offset 50 dB).

Redistribution subject to ASA license or copyright; see http://acousticalsociety.org/content/terms. Download to IP: 132.174.255.116 On: Thu, 27 Nov 2014 08:02:32

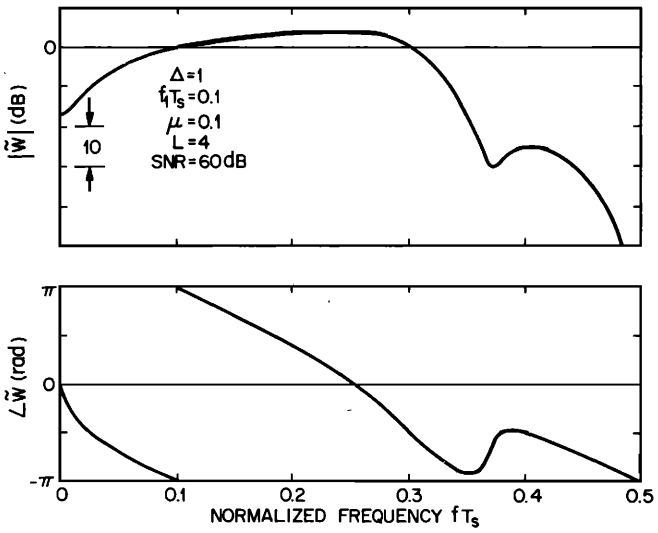

FIG. 12. Adapted gain and phase of $\tilde{W}(e^{j2\pi fT_s})$ (same parameter values as Fig. 9).

bit noise level (about −120 dB).

The SNR is 60 dB for the simulations shown in Figs. 9 and 10, yet the adapted residual volume velocities are clearly different (they are −55.5 and −30.3 dB, respectively). This behavior can be clarified by looking at spectra of the signals u_k, $\hat{u}_k$, and ur_k together with the adapted transfer functions $\tilde{W}$ and $\tilde{H}$ [Eqs. (19) and (20)]. Spectra and transfer functions corresponding to Fig. 9 (f_1T_s=0.1) are shown in Figs. 11–13, while those corresponding to Fig. 10 (f_1T_s=0.45) are shown in Figs. 14–16. All spectra were obtained using an FFT with the 512 data values immediately following the maximum value of $k=t_k/T_s$ shown in Figs. 9 and 10. A −90 dB (all side lobes guaranteed to be 90 dB or more below mainlobe amplitude) optimum data window[27] was used to minimize leakage in the spectrum of the sinusoid and to smooth slightly the random portions of the spectra.

The flat spectra of u_k (Figs. 11 and 14) illustrate the

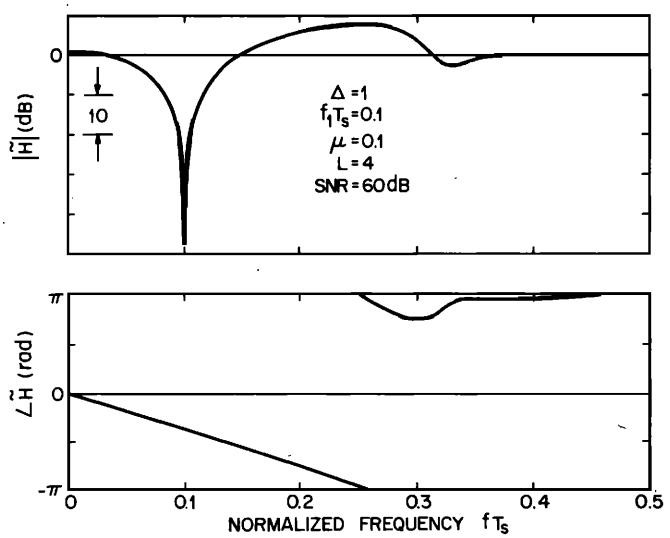

FIG. 13. Adapted gain and phase of $\tilde{H}(e^{j2\pi fT_s})$ (same parameter values as Fig. 9).

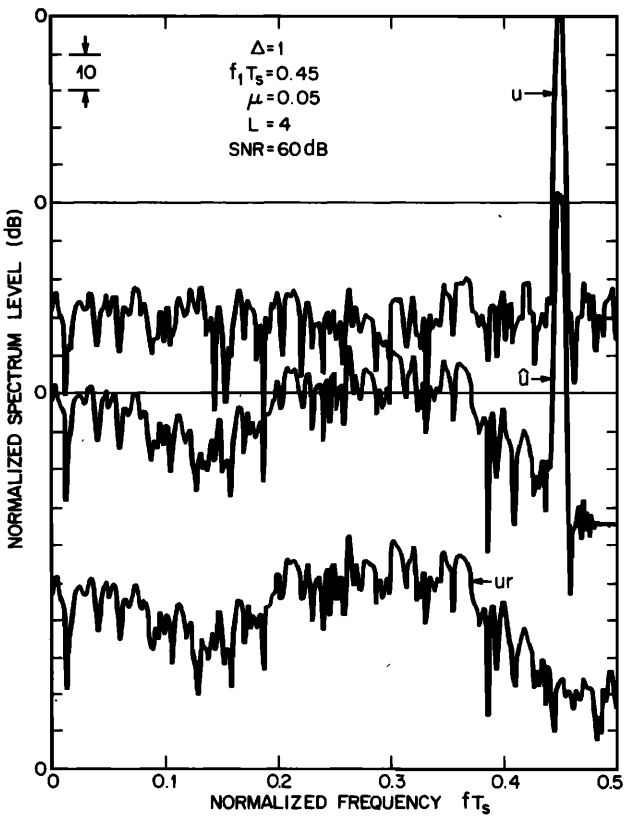

FIG. 14. Adapted FFT spectra of u_k, $\hat{u}_k$, and ur_k for f_1T_s=0.45 (same parameter values as Fig. 10; ordinates offset 50 dB).

white nature of the random noise subroutine used. The spectra for $\hat{u}_k$ and ur_k, however, show strongly colored (i.e., correlated) random noise. An eyeball comparison of these spectra with the corresponding transfer function gains for $\tilde{W}$ and $\tilde{H}$ (Figs. 12, 13 and 15, 16) shows that the coloration results from the noise passed by the filter $\tilde{W}$. It is also clear from the spectrum of ur_k in Fig. 11 that the sinusoid in u_k has been attenuated by at least 100 dB.

The adaptive filter W has two operating aspects. The

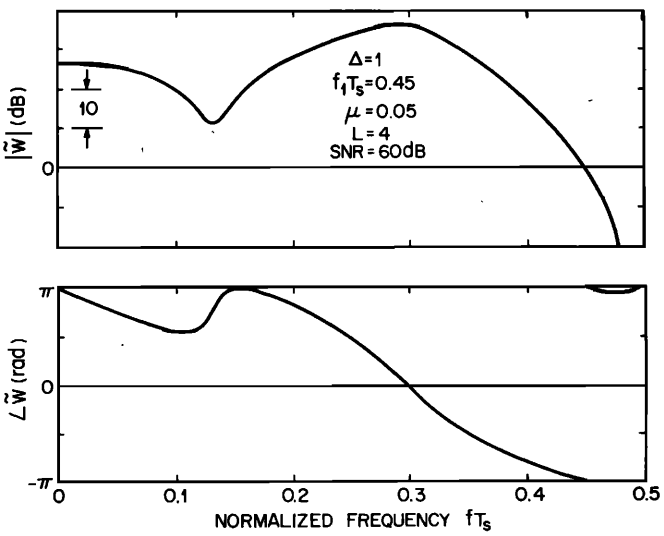

FIG. 15. Adapted gain and phase of $\tilde{W}(e^{j2\pi fT_s})$ (same parameter values as Fig. 10).

Redistribution subject to ASA license or copyright; see http://acousticalsociety.org/content/terms. Download to IP: 132.174.255.116 On: Thu, 27 Nov 2014 08:02:32

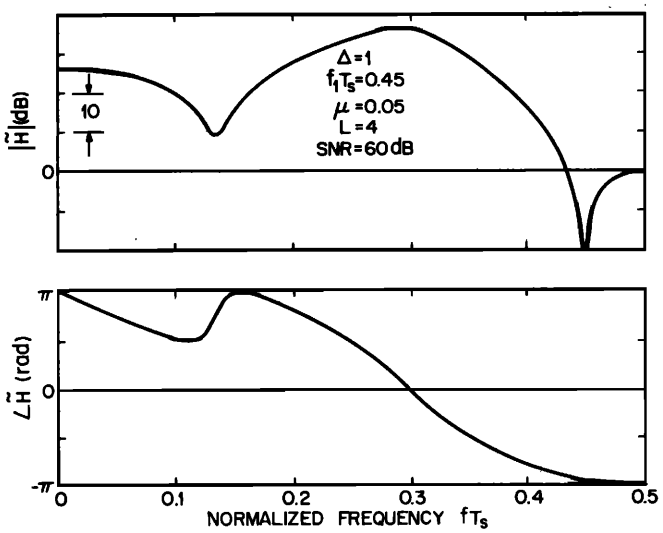

FIG. 16. Adapted gain and phase of $\tilde{H}(e^{j2\pi fT_s})$ (same parameter values as Fig. 10).

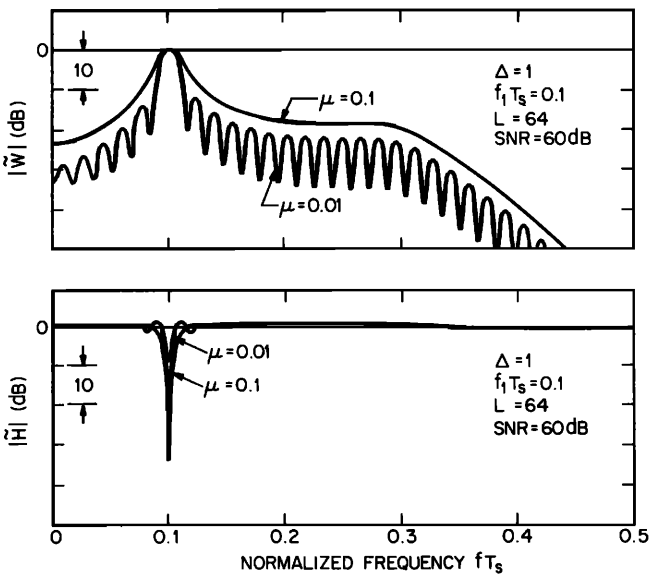

FIG. 18. Typical adapted gains of $\tilde{W}(e^{j2\pi fT_s})$ and $\tilde{H}(e^{j2\pi fT_s})$.

first is that it self selects its coefficients so that the adapted filter $\tilde{W}$ has the proper gain/phase at the sinusoid's frequency (0 dB/π for this simulation; see, e.g., Fig. 12 at $fT_s=0.1$). The second is that it acts as one or more bandpass filters with respect to the noise components in the training signal, x_k (see, e.g., the passband $0.1 \lesssim fT_s \lesssim 0.3$ in Fig. 12). To obtain the former, we must accept the latter when we use the configuration of Fig. 6.

There are at least two ways to decrease the noise contributions of $\hat{u}_k$ to the residual ur_k. One is to use a "clean" training signal, one that has components corresponding only to the correlated part of u_k. This would require a way to acquire x_k different from that shown in Fig. 6. Another way is to increase the length of W beyond the minimum required.

The adaptive filter W having the minimum required length, $L_{\min}$ functions by placing zeros of $\tilde{H}(z)$ where there are poles of $S(z)$, the correlated portion of $U(z)$. When s_k consists of one or more sinusoids, a minimum of two coefficients w_i is required for each (recall that each sinusoid can be thought of as the impulse response of a second order undamped system). Thus

$$L_{\min}=2N, \tag{25}$$

where N is the number of sinusoids in the training signal.

When the length of the adaptive filter is taken greater than the minimum, several things happen. One is that the adaptation rate changes (Fig. 17).

The adaptation rates shown in Fig. 17 were measured as slopes on plots of NR versus k (e.g., Fig. 9). A characteristic of these plots for a single sinusoid is that those for small L exhibit a predominantly linear (in semilog coordinates) portion while those for large L are curved, concave downwards. The values shown in Fig. 17 represent the slopes of the linear portions for small L and an estimate of the maximum slope for large L. The only aspects of Fig. 17 of significance are the marked decrease in adaptation time for L only slightly greater than $L_{\min}=2$, and the robustness of the maximum rate with respect to further increases in L. Specifically, the slight increase in adaptation time shown for large L may be due to measurement error.

The adaptation rates discussed in this paper all concern

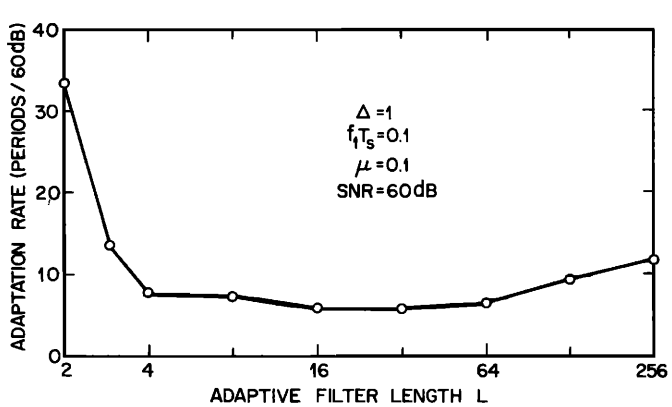

FIG. 17. Approximate adaptation rate of NR for a single sinusoid (same parameter values as Fig. 9).

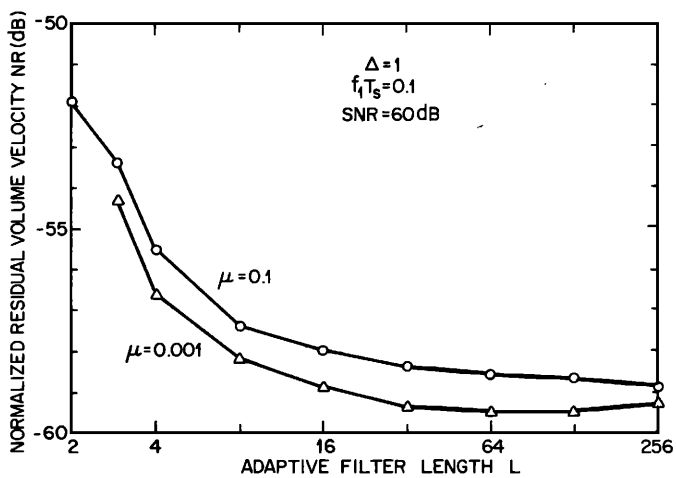

FIG. 19. Approximate adapted residual noise level with a single sinusoid in u_k.

Redistribution subject to ASA license or copyright; see http://acousticalsociety.org/content/terms. Download to IP: 132.174.255.116 On: Thu, 27 Nov 2014 08:02:32

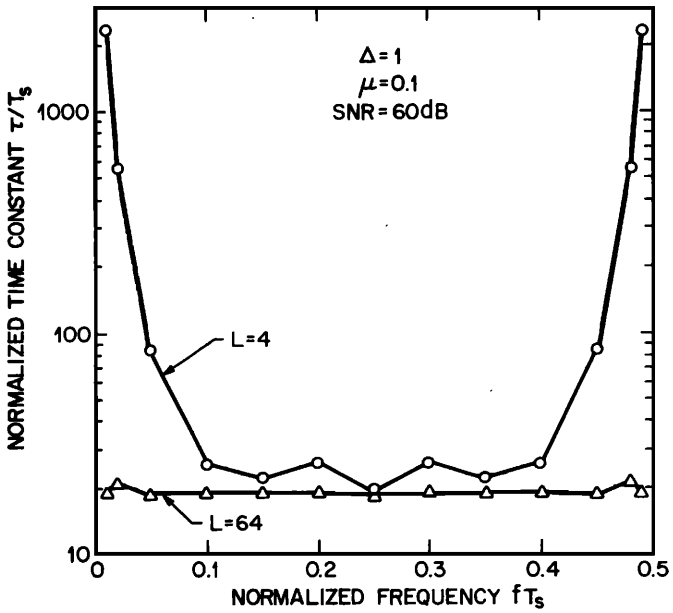

FIG. 20. Approximate adaptation rates of NR for a single sinusoid, $0 \leq f_1 T_s \leq 0.5$; $H2$ and $H3$ all-pass (unit gain, zero phase delay) filters.

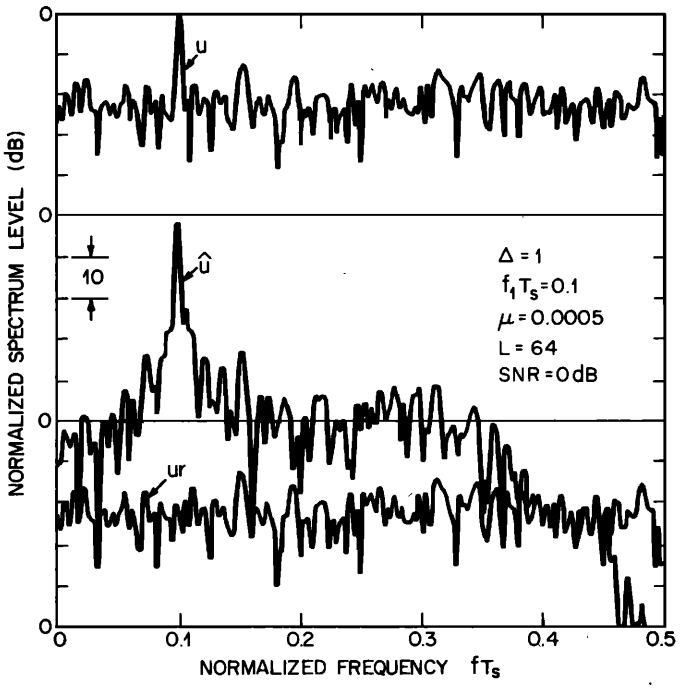

FIG. 22. FFT spectra of u_k, $\hat{u}_k$, and ur_k after adaptation for SNR = 0 dB (ordinates offset 50 dB).

NR. Another kind of adaptation rate concerns the coefficients $w_{k,l}$. Treichler[21] has discussed the latter in some detail. The two are related in that they are aspects of the same problem. They are different in that the former concerns adaptation of both amplitude and phase of a result, while the latter concerns adaptation of individual system parameters. No mathematical relations between the two kinds of adaptation appear to have been developed.

The second thing that happens when $L > L_{\min}$ is that the increased length allows the adaptive filter to position additional zeros in $\tilde{W}(z)$ and $\tilde{H}(z)$. The adaptive process places these zeros so that the gain of the transfer function $\tilde{W}$ more closely approximates the spectrum of the correlated components in u_k. The filter W, and thus $\tilde{W}$, approaches a high Q filter with center frequency at the frequency of the sinusoid in u_k. Comparison of the gains in Figs. 12 and 18 shows this effect clearly.

The increasing Q of filters W and $\tilde{W}$ with increasing L has a significant effect on reducing the power in the uncorrelated components of u_k that these filters pass (Fig. 19). The result of reducing the uncorrelated noise power transmitted by $\tilde{W}$ is that the residual spectrum and power more closely duplicate those of the relatively uncorrelated components in u_k. If $\Delta = 1$, which is the case here, the adaptive process tries to make the residual spectrum white. An example can be

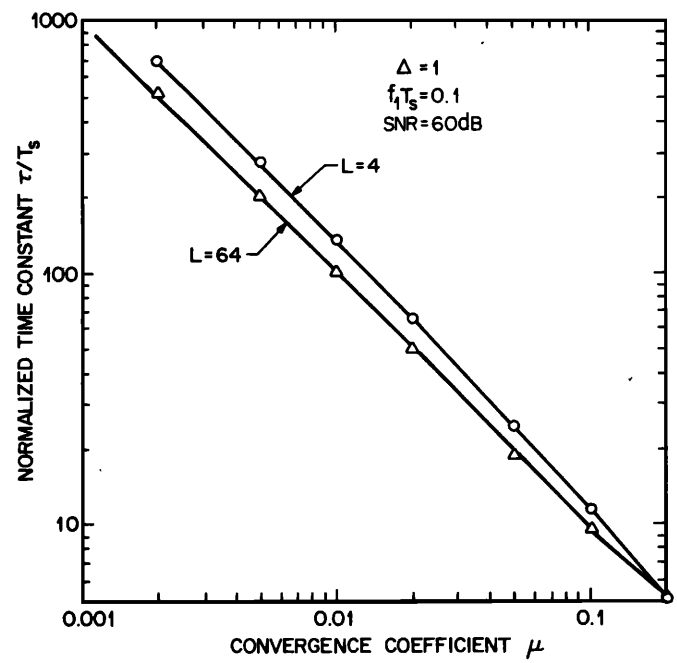

FIG. 21. Typical approximate adaptation rates of NR for a single sinusoid, $f_1 T_s = 0.1$, $H2$ and $H3$ all-pass (unit gain, zero phase delay) filters.

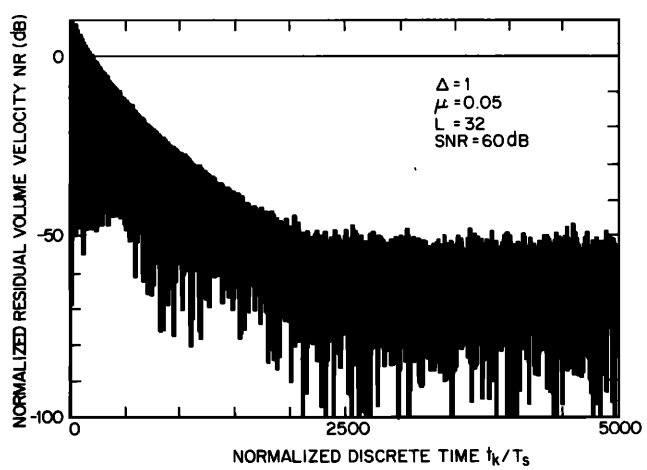

FIG. 23. Simulated normalized residual volume velocity versus discrete time for five equal-amplitude sinusoids, $f_n T_s = 0.04, 0.12, 0.20, 0.28, 0.36$.

Redistribution subject to ASA license or copyright; see http://acousticalsociety.org/content/terms. Download to IP: 132.174.255.116 On: Thu, 27 Nov 2014 08:02:32

seen by comparing the spectra for ur in Figs. 11 and 22.

A third thing that happens when $L > L_{min}$ is hidden in the adaptation process. The coefficient of W_k and the forcing term in Eq. (11a) are both time dependent. There are two kinds of time dependency; that during the convergence process and that following adaptation. During the convergence process when u_k includes sinusoids, additional sinusoids are generated.[28] These appear in both $\hat{u}_k$ and ur_k. They result in at least an increased convergence time and at worst instability. Increasing L can decrease convergence time (Fig. 20). Note the symmetry in Fig. 20 of adaptation rates[28] about $f T_s = 0.25$.

Following adaptation, the LMS algorithm causes the coefficients $w_{k,l}$ to hunt about their mean value. This, in turn, causes the locations of adaptive zeros in $\tilde{W}$ and $\tilde{H}$ to vary relative to their mean positions. The resulting time dependency of the transfer functions $\tilde{W}$ and $\tilde{H}$ causes a modulation of both the correlated and uncorrelated components in u_k. The effects are called *weight vector noise*. These effects can be reduced by using smaller values of μ.

Another effect of using smaller μ is that the filter $\tilde{W}$ at any time k after adaptation has a higher Q. Figure 18 shows an example of increased Q with smaller μ. It also shows that smaller μ results in repositioning the zeros of $\tilde{W}$ closer to the unit circle.

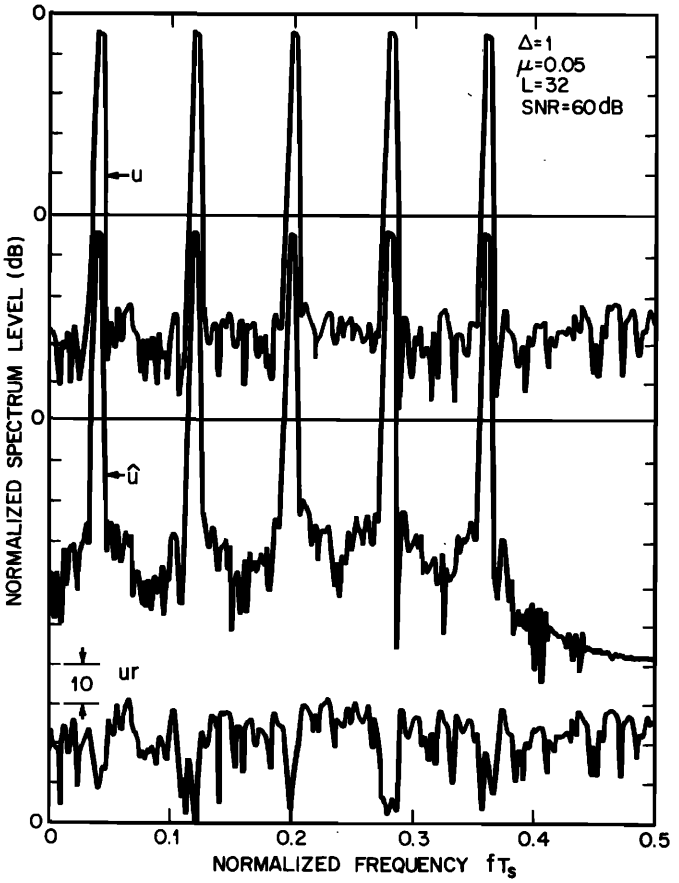

FIG. 24. Adapted FFT spectra of u_k, $\hat{u}_k$, and ur_k (after k = 5000) for five equal-amplitude sinusoids, (same parameter values as Fig. 23; ordinates offset 50 dB).

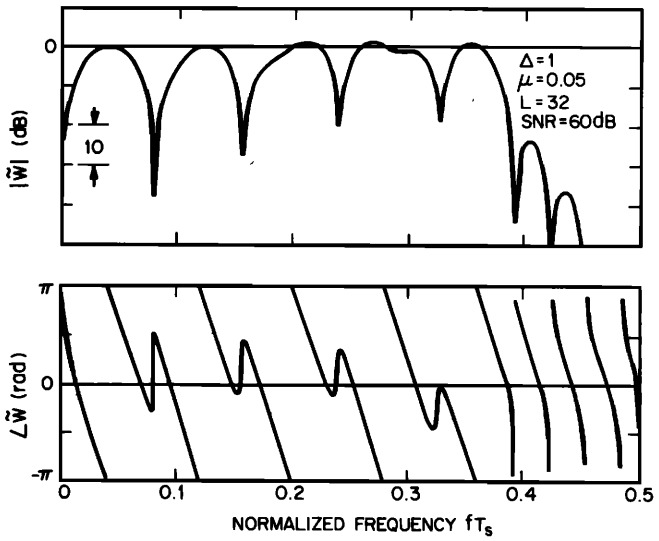

FIG. 25. Adapted gain and phase of $\tilde{W}(e^{j2\pi fT_s})$ (same parameter values as Fig. 23).

Figure 19 shows that smaller μ results in decreased residual noise level. This decrease is attributable to both the higher Q of $\tilde{W}$ (time-invariant properties of W) and decreased weight vector noise (time varying properties of W).

From the foregoing discussion, the parameter μ can be seen to have a variety of effects. They all have a common base in that the adaptive filter must have time dependent coefficients. A primary effect of making μ smaller is to reduce the adaptation rate. Typical values for adaptation rate are shown in Figs. 20 and 21 (time constant τ is time to decrease by $1/e$).

Adaptation can take place even when the broadband noise, n_k, is dominant (e.g., SNR $\simeq -10$ dB). Satisfactory adaptation requires that the weights $w_{k,l}$ approach and remain near their optimum values, w_l^*. For low SNR, this requires a combination of small values of μ and large values of L. Small μ reduces weight vector noise. Large L results in a high Q filter $\tilde{W}$, which reduces the noise passed by $\tilde{W}$. Spectra for u, $\hat{u}$, and ur are shown in Fig. 22 after adaptation for SNR = 0 dB. Note the total absence of the sinusoid from the spectrum of ur.

Adaptation will take place when there are multiple sinusoids in u_k. Figures 23–26 show results when there are five sinusoids of equal amplitude. When the sinu-

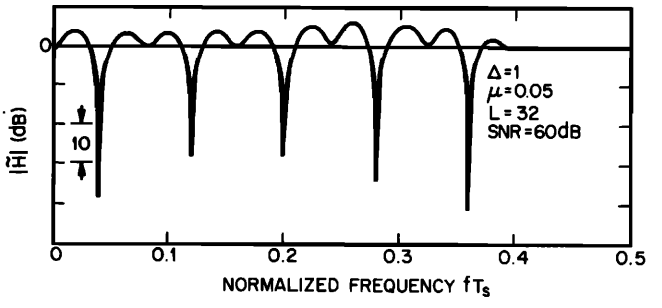

FIG. 26. Adapted gain of $\tilde{H}(e^{j2\pi fT_s})$ (same parameter values as Fig. 23).

Redistribution subject to ASA license or copyright; see http://acousticalsociety.org/content/terms. Download to IP: 132.174.255.116 On: Thu, 27 Nov 2014 08:02:32

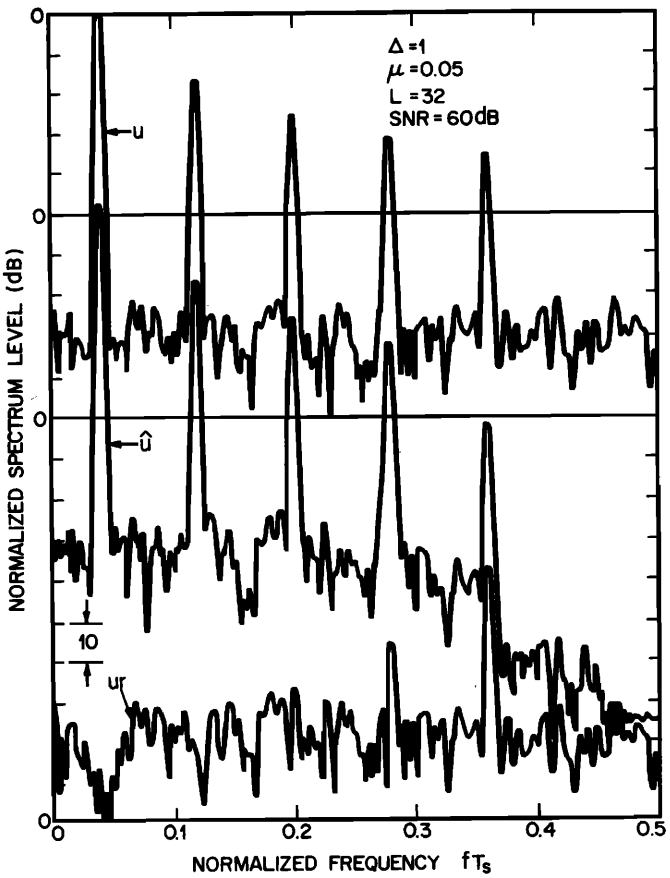

FIG. 27. FFT spectra of u_k, $\hat{u}_k$, ur_k after $k = 50\,000$ for the first five components of a triangular wave, $f_n T_s = 0.04$, 0.12, 0.20, 0.28, 0.36 (ordinates offset 50 dB).

soids are of unequal amplitude, the system of Fig. 6 with Eq. (23a) adapts more rapidly to the high-amplitude harmonics than to the low-amplitude harmonics. Some partial results of simulation with the first five components of a triangular wave are shown in Fig. 27. Adaptation after 50 000 iterations is continuing very slowly. These results suggest that a training signal having clean sinusoids of equal amplitude is preferable to one which duplicates the amplitudes in the signal to be canceled.

During the development of the computer simulation of Fig. 6, $H2$, $H3$, and $H4$ were first simulated by pure delays with u_k a single sinusoid. With $H4$ a zero delay, the adaptive filter update system remained stable as long as the sum of the delays of H_2 and $H3$ was less than a quarter period of the sinusoid. This result agrees with those reported by Morgan.[29] When $H4$ was simulated as a delay equal to the sum of the delays in $H2$ and $H3$, the instabilities disappeared. No instabilities corresponding to those reported by Morgan were observed in the computer simulation of the system of Fig. 6 with Eq. (23a). Morgan's Fig. 1(b) implies that the equivalent of $H4$ was absent from his realization. His results thus provide important insight into the effects of errors in the phase delay of $H4$ on stability of the adaptive filter update system. A practical application of these results is that $H4$ [Eq. (22c)] need not exactly duplicate the sum of the phase delays of $H2$ and $H3$ to preserve stability. Generating an $H4$ of suitable accuracy for a practical realization will require real system identification and modeling.

A primary advantage of a closed-loop system over an open-loop system is that it can adjust to changes in uncontrollable system parameters. The adaptation rates shown in Figs. 17, 20, and 21 provide a rough measure of the maximum rates of change in single tone amplitude that this adaptive process can track. Griffiths[25] has shown that the LMS adaptive algorithm can also track changes in frequency, provided they are not too rapid.

VI. CONCLUSIONS

The principle of the adaptive noise canceler can be successfully extended from signal processing to control applications. Simulation results imply that the use of an LMS adaptive algorithm with existing noise cancellation systems can improve and extend their practical applicability. The active adaptive sound controller can be designed to accommodate gain and phase changes introduced by fixed system elements as well as to accomodate slow variations of amplitude and frequency of the sound to be canceled. The method can be applied more widely to control systems which involve transport delay.

ACKNOWLEDGMENTS

This work was performed at Bell Laboratories while I was on sabbatical leave from the University of Hawaii. I am indebted to J. L. Flanagan for making it possible and to many colleagues in the Acoustics Research Department for friendly support. I particularly thank Mohan Sondhi and David Malah for stimulating discussions about adaptive signal processing and for helpful early reviews of the manuscript. I thank also other unknown reviewers at Bell Laboratories and in the Society for their constructive comments. The paper incorporates results presented at a Society meeting.[30]

[1]C. M. Harris and C. T. Molloy, "The theory of sound absorptive materials," J. Acoust. Soc. Am. 24, 1–7 (1952).
[2]H. F. Olson and E. G. May, "Electronic sound absorber," J. Acoust. Soc. Am. 25, 1130–1136 (1953).
[3]B. D. Tartakovsky, "On vibration and sound field compensation methods using multichannel systems," paper F–5–14, The 6th International Congress on Acoustics, Tokyo (1968).
[4]M. J. M. Jessel and G. A. Mangiante, "Active sound absorbers in an air duct," J. Sound Vib. 23, 383–390 (1972).
[5]M. A. Swinbanks, "The active control of sound propagation in long ducts," J. Sound Vib. 27, 411–436 (1973).
[6]G. Canévet and G. Mangiante, "Absorption acoustique active et anti-bruit à une dimension," Acustica 30, 40–48 (1974).
[7]H. G. Leventhall, "Developments in active attenuators," 1976 Noise Control Conference, Warsaw, 33–42 (1976).
[8]J. H. B. Poole and H. G. Leventhall, "An experimental study of Swinbanks' method of active attenuation of sound in ducts," J. Sound Vib. 49, 257–266 (1976).
[9]J. H. B. Poole and H. G. Leventhall, "Active attenuation of noise in ducts," J. Sound Vib. 57, 308–309 (1978).
[10]"Active silencer for low-frequency noise," J. Acoust. Soc. Am. 66, 1215 (1979).

Redistribution subject to ASA license or copyright; see http://acousticalsociety.org/content/terms. Download to IP: 132.174.255.116 On: Thu, 27 Nov 2014 08:02:32

[11]"Active Control of Sound Waves," U.S. Patent 4,044,203, reviewed in J. Acoust. Soc. Am. 63, 1958 (1978); 66, 1577 (1979).
[12]G. A. Mangiante, "Active sound absorption," J. Acoust. Soc. Am. 61, 1516–1523 (1977) (note: has extensive bibliography).
[13]O. L. Angevine, P. K. Gupta, and F. A. Rushden, "Active acoustic absorbers for low-frequency hum," J. Acoust. Soc. Am. Suppl. 1,67, S86 (1980).
[14]T. Angelini and G. Capolino, "Sur le pilotage d'absorbeurs acoustiques actifs," paper F–41, Ninth International Congress on Acoustics, Madrid (1977).
[15]S. Onoda and K. Kido, "Automatic control of stationary noise by means of directivity synthesis," paper F–5–13. The 6th International Congress on Acoustics, Tokyo (1968).
[16]M. M. Sondhi, "An adaptive echo canceller," Bell Syst. Tech. J. 46, 467–511 (1967).
[17]B. Widrow *et al.*, "Adaptive noise cancelling: principles and applications," Proc. IEEE 63, 1692–1716 (1975).
[18]L. E. Kinsler and A. R. Frey, *Fundamentals of Acoustics* (Wiley, New York, 1962), 2nd ed., Chap. 8.
[19]P. M. Morse and K. U. Ingard, *Theoretical Acoustics* (McGraw–Hill, New York, 1968), pp. 489–90.
[20]M. M. Sondhi and D. A. Berkley, "Silencing echoes on the telephone network," Proc. IEEE 68, 948–963 (1980).
[21]J. R. Treichler, "Transient and convergent behavior of the adaptive line enhancer," IEEE Trans. Acoust. Speech Signal Proc. ASSP–27, 53–62 (1979).
[22]B. Widrow, "Adaptive Filters," in *Aspects of Network and System Theory*, edited by R. E. Kalman and H. DeClaris (Holt, Rinehart and Winston, New York, 1971).
[23]D. G. Childers, *Modern Spectrum Analysis* (The Institute of Electrical and Electronic Engineers, New York, 1978).
[24]J. Makhoul, "Linear prediction: a tutorial review," Proc. IEEE 63, 561–580 (1975), reprinted in Ref. 23.
[25]L. J. Griffiths, "Rapid measurement of digital instantaneous frequency," IEEE Trans. Acoust. Speech Signal Proc. ASSP –23, 207–222 (1975), reprinted in Ref. 23.
[26]A. Nehorai and D. Malah, "On the stability and performance of the adaptive line enhancer," Proc. Int. Conf. Acoust. Speech Signal Proc. Denver, 478–481 (9–11 April 1980).
[27]J. C. Burgess, "Approximations to Dolph-Chebyshev data windows," J. Acoust. Soc. Am. Suppl. 1,65, S61 (1979).
[28]J. R. Glover, "Adaptive noise cancelling applied to sinusoidal interferences," IEEE Trans. Acoust. Speech Signal Proc. ASSP–25, 484–491 (1977).
[29]D. R. Morgan, "An analysis of multiple correlation cancellation loops with a filter in the auxiliary path," IEEE Trans. Acoust. Speech Signal Proc. ASSP–28, 454–467 (1980).
[30]J. C. Burgess, "Active adaptive 'Helmholtz resonator'," J. Acoust. Soc. Am. Suppl. 1,68, S91–92 (1980).

Redistribution subject to ASA license or copyright; see http://acousticalsociety.org/content/terms. Download to IP: 132.174.255.116 On: Thu, 27 Nov 2014 08:02:32